# EASTLAND PORT MAINTENANCE DREDGING AND DISPOSAL PROJECT

## Establishment of empirical equations to predict long period wave climate at berth

Report prepared for Eastland Port

February 2018

MetOcean SOLUTIONS

MetOcean Solutions Ltd: P0331 - 09

February 2018

Report status

| Version | Date | Status | Approved by |
|---|---|---|---|
| RevA | 19/02/2018 | Draft for internal review | Monetti |
| RevB | 22/02/2018 | Draft for client review | Beamsley |
| | | | |
| | | | |

It is the responsibility of the reader to verify the currency of the version number of this report.

**TABLE OF CONTENTS**

## LIST OF FIGURES

**LIST OF TABLES**

# 1. INTRODUCTION

Eastland Port Ltd are seeking to renew their maintenance dredging and disposal consents at the Port of Gisborne.

Currently, dredged sediment is disposed at an offshore disposal site situated in approximately 18 – 20 m water depth (**Error! Reference source not found.**), with an average annual rate of approximately 73,000 $m^3$ based on estimates obtained between 2002 and 2019 by Eastland Port.

Maintenance dredging is expected to occur using the Trailing Suction Hopper Dredge (TSHD) “Pukunui” although, if there are significant inflows of sediment due to large storm events, a higher productivity Trailing Suction Hopper Dredge (TSHD) may be required to ensure the required port and channel depths can be maintained. It is likely that some maintenance dredging may also be undertaken using a Backhoe Dredger (BHD) or Cutter Suction Dredger (CSD).

MetOcean Solutions (MOS) has been contracted to establish a set of empirical equations to predict long period wave (LPW) climate along berth sites to optimise maintenance dredging design. For this purpose, outputs from the Boussinesq wave model FUNWAVE have been used to rescale the existing equation defined in the operational forecast system for specific site in the harbour.

The complete methodology is presented in Section 2, including the description of the techniques and datasets used to predict the LPW climate into the harbour. The predicted long period wave climate at berth sites is provided in Section 3 while some recommendations are given in Section 4 and a brief summary in Section 5.

Note that some additional required information is provided in Appendix for completeness.

# 2. METHODS

## 2.1. Background

Long period (or infragravity) waves are water level oscillations with periods of greater than 25 s. These waves are of consequence to harbour and marine terminal operations because they can energise moored vessels – potentially inducing problematic ranging and surging motions. Furthermore, these long period waves have the potential to lower the water level and impact vessel underkeel clearance requirements. The frequency band corresponding to 25-150 s period is the most significant as the moored vessels' resonant response typically lies within this range. This range also coincides with the dominant frequencies that arise from the non-linear transfer of sea-swell energy into longwaves during the nearshore wave transformation process (Thomson et al., 2006; Holthuijsen, 2010).

## 2.2. Empirical LPW equation used in the forecast system at Eastland Port

In previous work, MetOcean Solutions have established an empirical equation to forecast LPW within Eastland Port by analysing the statistical parameters of sea-swell waves in Poverty Bay as well as the tide variation.

Measured and predicted LPW data were compared at a reference site IG (see Table 2.1 and Figure 2.1) in the harbour to obtain a LPW predictor (Eq. 2.1) estimated from non-linear least square regression adjusted with tidal variation.

$$H_{s\,(LPW)} = (1 + 0.54\,\eta_{tide})\left(0.011\,{H_{s\,(swell)}}_{off}^{1.1}\,{T_p}_{off}^{0.5} + 0.025\right)$$

Eq. 2.1

where:

$H_{s\,(LPW)}$ is the significant LPW height (in meters) at the IG site,

$\eta_{tide}$ is the tidal level (in meters) from Chart Datum (CD),

${H_{s\,(swell)}}_{off}$ is the significant swell wave height (in meters) at the offshore site,

${T_p}_{off}$ is the spectral peak period of sea-swell height (in seconds) at the offshore site.

## 2.3. Boussinesq wave data

In the past, MetOcean Solutions have carried out a set of simulations over northern Poverty Bay and Eastland Port using the Boussinesq FUNWAVE model to capture the generation and propagation of LPW energy into the harbour (MetOcean Solutions, 2013). Five hourly wave events at both low and high tides have been simulated using bi-directional spectral boundary conditions (10-simulations in total). The established numerical model has been successfully validated comparing $H_{s(LPW)}$ against measurements within the harbour.

In the present study, we proposed to use these model data to examine the ratio between $H_{s(LPW)}$ at Site IG and along berth to rescale the previously established empirical equation.

The primary model output was the instantaneous surface elevation, stored at 1 second intervals. Here, the instantaneous surface elevation have been extracted at 19 sites within the harbour (Table 2.1) and then analysed using a zero-crossing method to calculate $H_{s\_swell}$ and $H_{s(LPW)}$ based on the following frequency bands:

0.040 – 0.125 Hz (total LPW band 25 s period and above)

0.005 – 0.040 Hz (Swell band between 8 s and 25 s)

Note that these frequency bands were defined base on those previously used to forecast LPW in Eq. 2.1. The peak period $T_p$ was extracted from the instantaneous surface elevation using a Fast Fourier Transform (FFT).

## 2.4. Extension of the LPW empirical equation to berth sites

In absence of LPW measurements at berth sites, the Boussinesq model outputs were used to determine relationships between $H_{s(LPW)}$ at Position IG and along berth using linear regression techniques. A set of 18 intermediate equations were thus defined as follows:

$$H_{s\,(LPW)_{site}} = a1\; H_{s\,(LPW)_{IG}}$$

Eq. 2.2

where coefficient *a1* vary with the location based on the Boussinesq model outputs.

The coefficient *a1* was then introduced in Eq. 2.1 to establish a set of empirical relationships to support the prediction of $H_{s\,(LPW)}$ at berth sites from $H_{s\,(swell)\,offshore}$, $T_p$ and the tidal variation. All new equations are presented in Section 3.2.

Table 2.1 Coordinates of the sites used in the present study to establish new empirical relationship between $H_{s\ (LPW)}$, $Hs_{\ (swell)\ offshore}$, $T_p$ offshore and the tidal elevation. The Site IG is the reference position where comparisons between model and measured data allowed establishing the original empirical equation from offshore wave conditions at Site WB.

| Position | Longitude (E) | Latitude (N) |
|---|---|---|
| **WB** | 178.012000 | -38.687000 |
| **IG** | 178.022110 | -38.675000 |
| **1** | 178.027517 | -38.672717 |
| **2** | 178.027048 | -38.672983 |
| **3** | 178.026571 | -38.673242 |
| **4** | 178.026104 | -38.673496 |
| **5** | 178.025626 | -38.673755 |
| **6** | 178.025154 | -38.674012 |
| **7** | 178.024682 | -38.674268 |
| **8** | 178.024215 | -38.674522 |
| **9** | 178.023737 | -38.674781 |
| **10** | 178.023265 | -38.675037 |
| **11** | 178.022798 | -38.675291 |
| **12** | 178.022321 | -38.675551 |
| **13** | 178.021861 | -38.675813 |
| **14** | 178.021396 | -38.676077 |
| **15** | 178.020926 | -38.676345 |
| **16** | 178.020462 | -38.676609 |
| **17** | 178.020194 | -38.676761 |
| **18** | 178.0262 | -38.6736 |

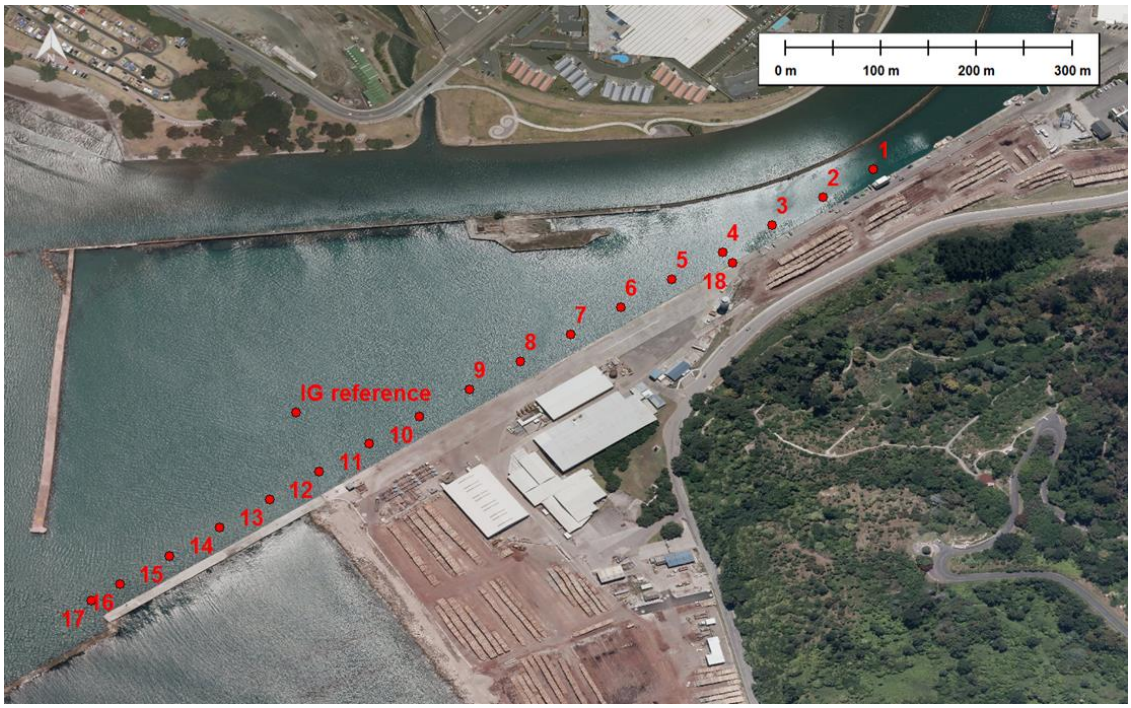


Figure 2.1 Location of the sites used in the present study to establish new empirical relationship between $H_{s\ (LPW)}$, $H_{s\ (swell)\ offshore}$, $T_p$ offshore and the tidal elevation. The Site IG is the reference where comparisons between model and measured data allowed establishing the original empirical equation.

## 2.5. Reconstruction of the LPW climate at berth sites

A reconstruction of the LPW climate at the berth sites was carried out applying the empirical equations established in the present study. Inputs were provided using nowcast wave data produced by MetOcean Solutions at Site WB between 2012 and 2017. Wave statistics including mean, maximum and percentiles p50, p95 and p99 were calculated from the different time series of $H_{s(LPW)}$ at each berth site. Results are provided in Section 3.3.

# 3. RESULTS

## 3.1. Empirical relationships between LPW at IG and along berth

The coefficient *a1* obtained by applying a linear regression to fit the values of $H_{s\ (LPW)\ site}$ and $H_{s\ (LPW)\ IG}$ from the Boussinesq model outputs are summarised in Table 3.1.

To ensure the validity of using *a1* to calibrate new empirical LPW equations, we examined the correlation between the values of $H_{s\ (LPW)}$ for the 10 scenarios obtained from FUNWAVE and the intermediate equation Eq. 2.2. The relative close values depicted in Figure 3.1 to Figure 3.9 highlighted a relative low degree of variability of the ratio $H_{s\ (LPW)\ site}$ / $H_{s\ (LPW)\ IG}$ between the different events, making possible the rescaling of the original LPW equation defined at Site IG. Some limitations in applying this approach are however discussed in Section 4.

Table 3.1 Equations at Positions 1 to 18 based on the wave conditions at the WB site.

| Position | Longitude (E) | Latitude (N) | Coefficient |
|---|---|---|---|
| | | | a1 |
| **IG** | 178.022110 | -38.675000 | - |
| **1** | 178.027517 | -38.672717 | 3.6253 |
| **2** | 178.027048 | -38.672983 | 3.5980 |
| **3** | 178.026571 | -38.673242 | 3.4123 |
| **4** | 178.026104 | -38.673496 | 2.8941 |
| **5** | 178.025626 | -38.673755 | 2.3542 |
| **6** | 178.025154 | -38.674012 | 1.9582 |
| **7** | 178.024682 | -38.674268 | 1.5960 |
| **8** | 178.024215 | -38.674522 | 1.4334 |
| **9** | 178.023737 | -38.674781 | 1.2692 |
| **10** | 178.023265 | -38.675037 | 1.1565 |
| **11** | 178.022798 | -38.675291 | 1.1255 |
| **12** | 178.022321 | -38.675551 | 1.2657 |
| **13** | 178.021861 | -38.675813 | 1.5091 |
| **14** | 178.021396 | -38.676077 | 1.7214 |
| **15** | 178.020926 | -38.676345 | 1.9267 |
| **16** | 178.020462 | -38.676609 | 2.1043 |
| **17** | 178.020194 | -38.676761 | 2.2478 |
| **18** | 178.026200 | -38.673600 | 2.9058 |

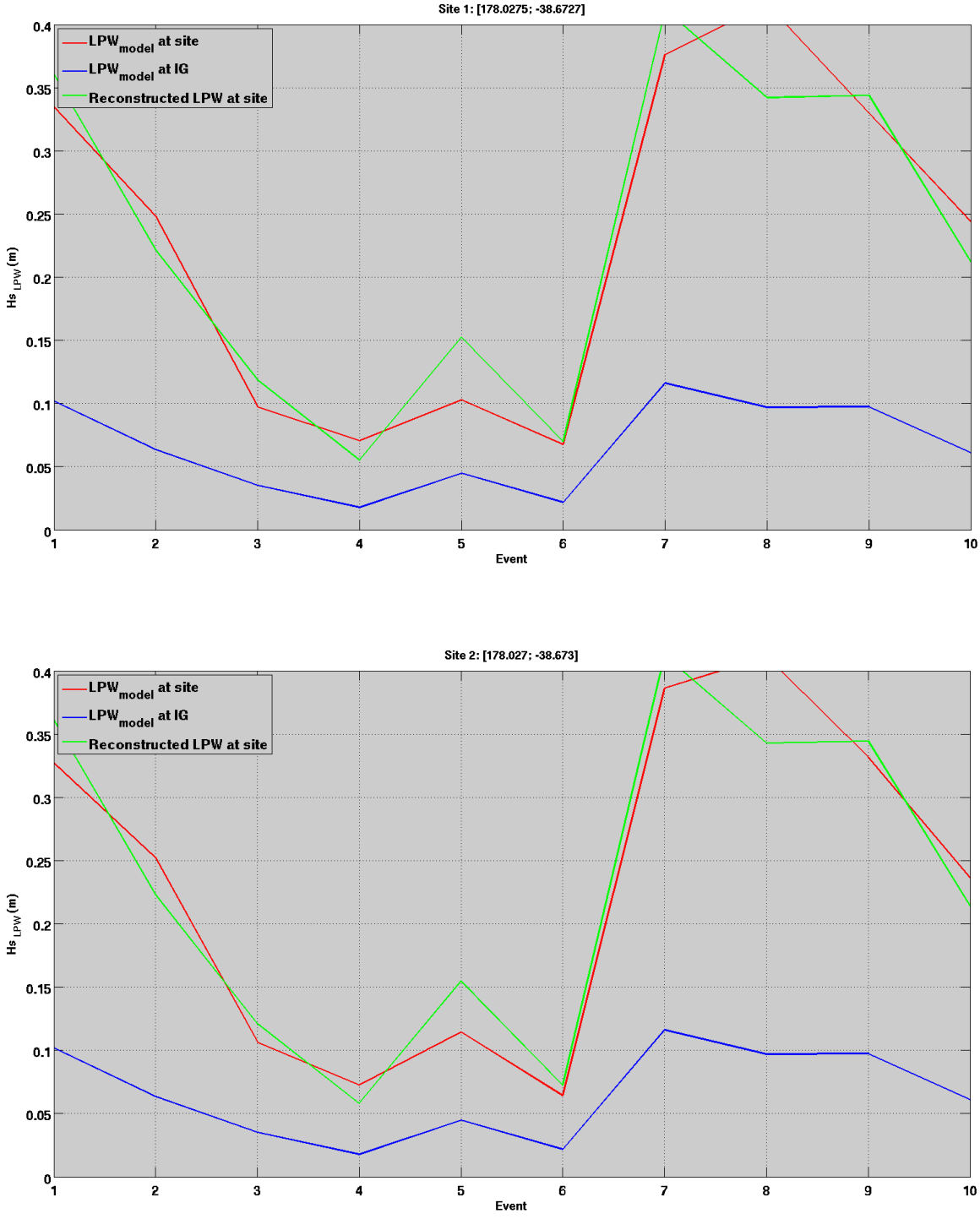


Figure 3.1 Model and reproduced $H_{s\ (LPW)}$ at Sites 1 and 2 for a total of 10 events (5 events at high and low tides) obtained from the Boussinesq wave model and the Equation 2.2, respectively,. The blue line indicates the model $H_{s\ (LPW)}$ at Site IG used in Equation 2.2.

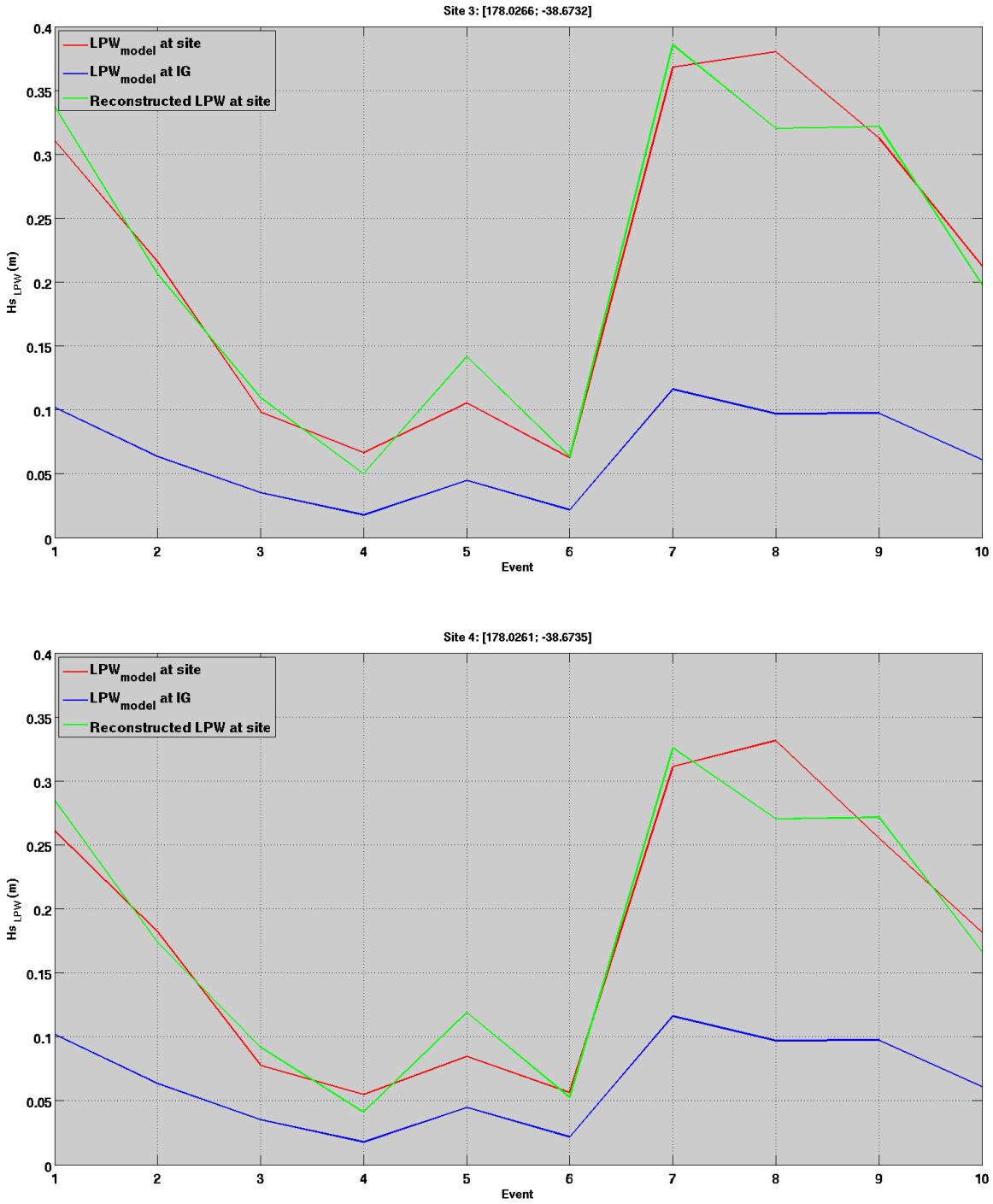


Figure 3.2 Model and reproduced $H_{s\ (LPW)}$ at Sites 3 and 4 for a total of 10 events (5 events at high and low tides) obtained from the Boussinesq wave model and the Equation 2.2, respectively,. The blue line indicates the model $H_{s\ (LPW)}$ at Site IG used in Equation 2.2.

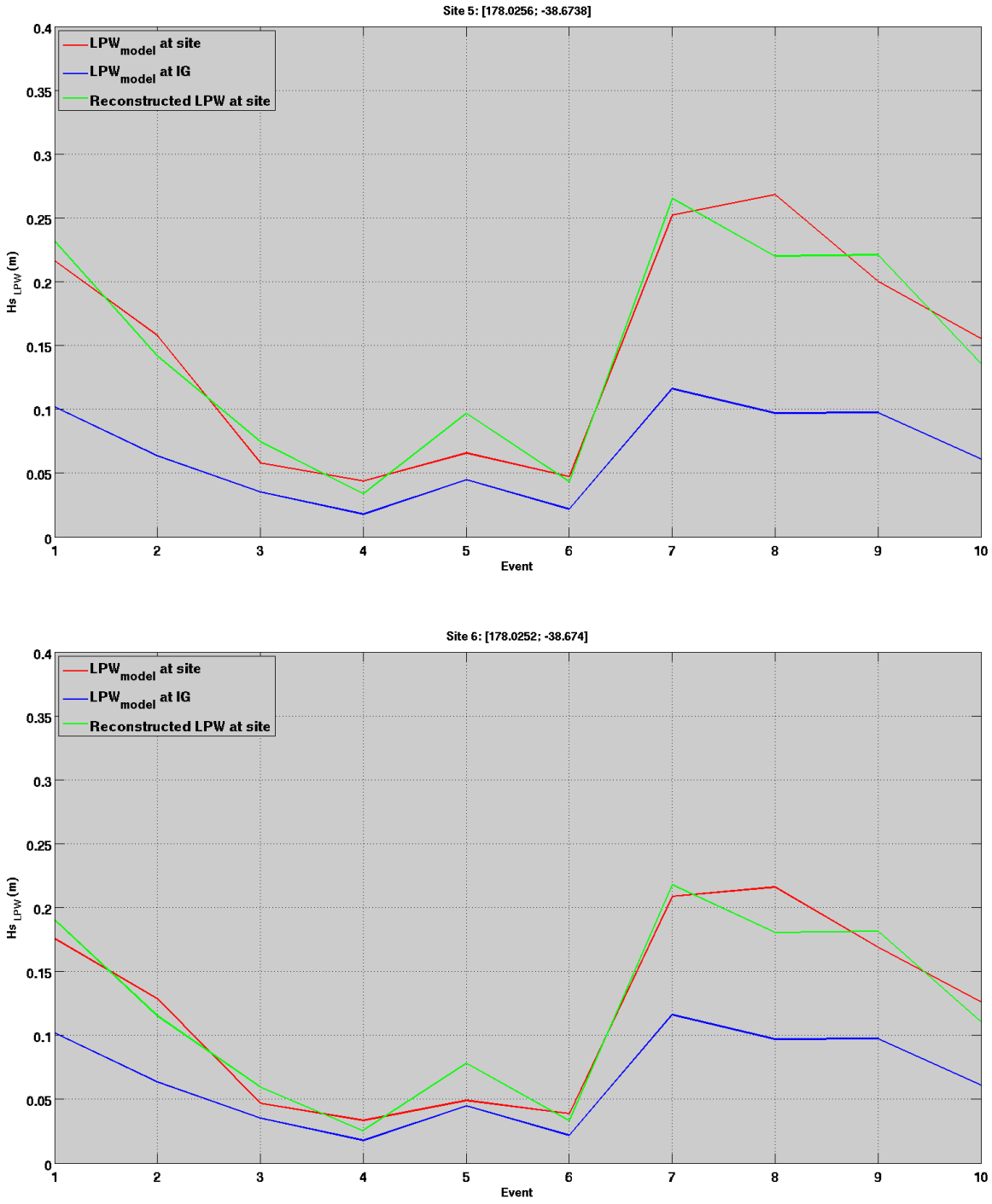


Figure 3.3 Model and reproduced $H_{s\ (LPW)}$ at Sites 5 and 6 for a total of 10 events (5 events at high and low tides) obtained from the Boussinesq wave model and the Equation 2.2, respectively,. The blue line indicates the model $H_{s\ (LPW)}$ at Site IG used in Equation 2.2.

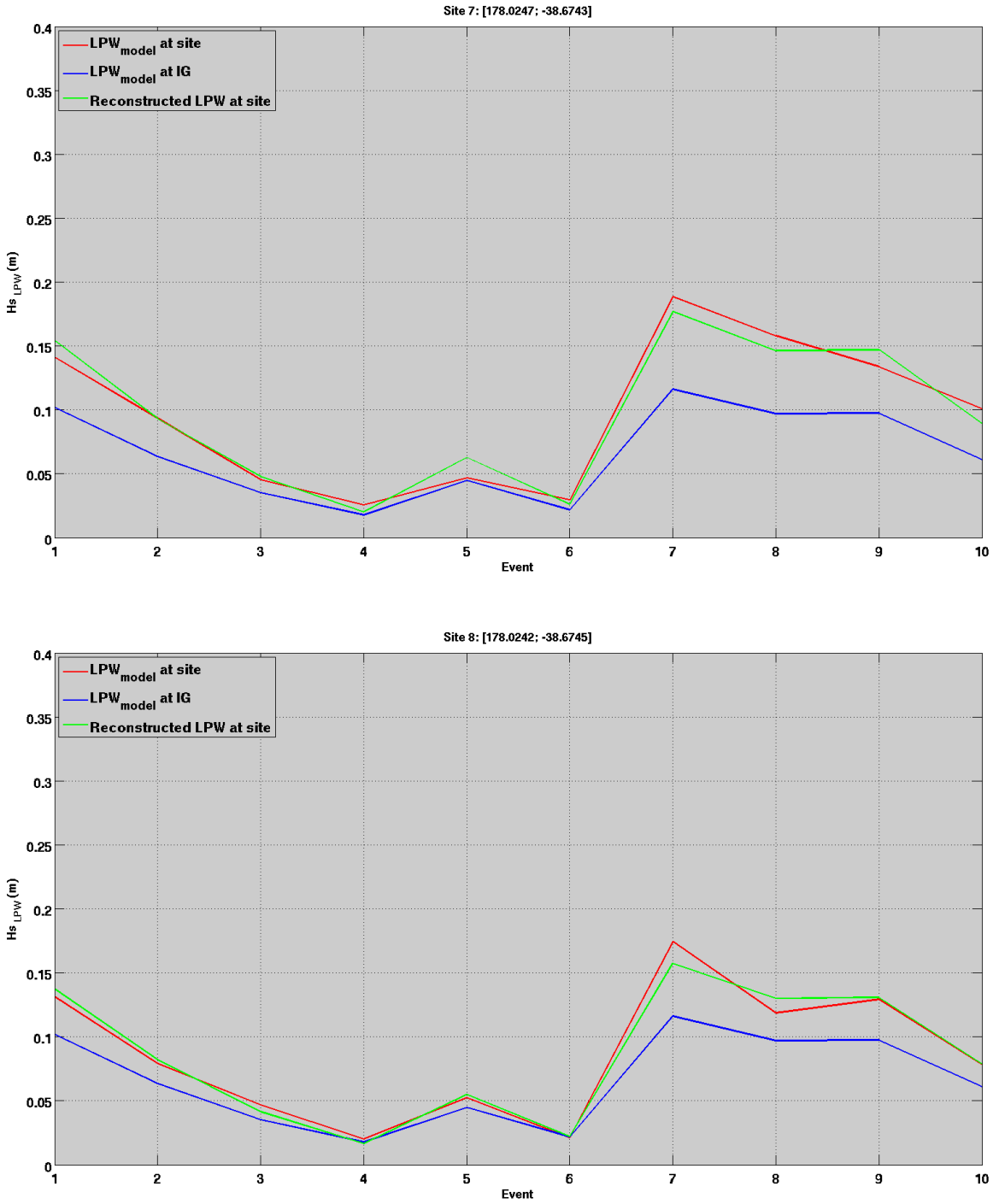


Figure 3.4 Model and reproduced $H_{s\ (LPW)}$ at Sites 7 and 8 for a total of 10 events (5 events at high and low tides) obtained from the Boussinesq wave model and the Equation 2.2, respectively,. The blue line indicates the model $H_{s\ (LPW)}$ at Site IG used in Equation 2.2.

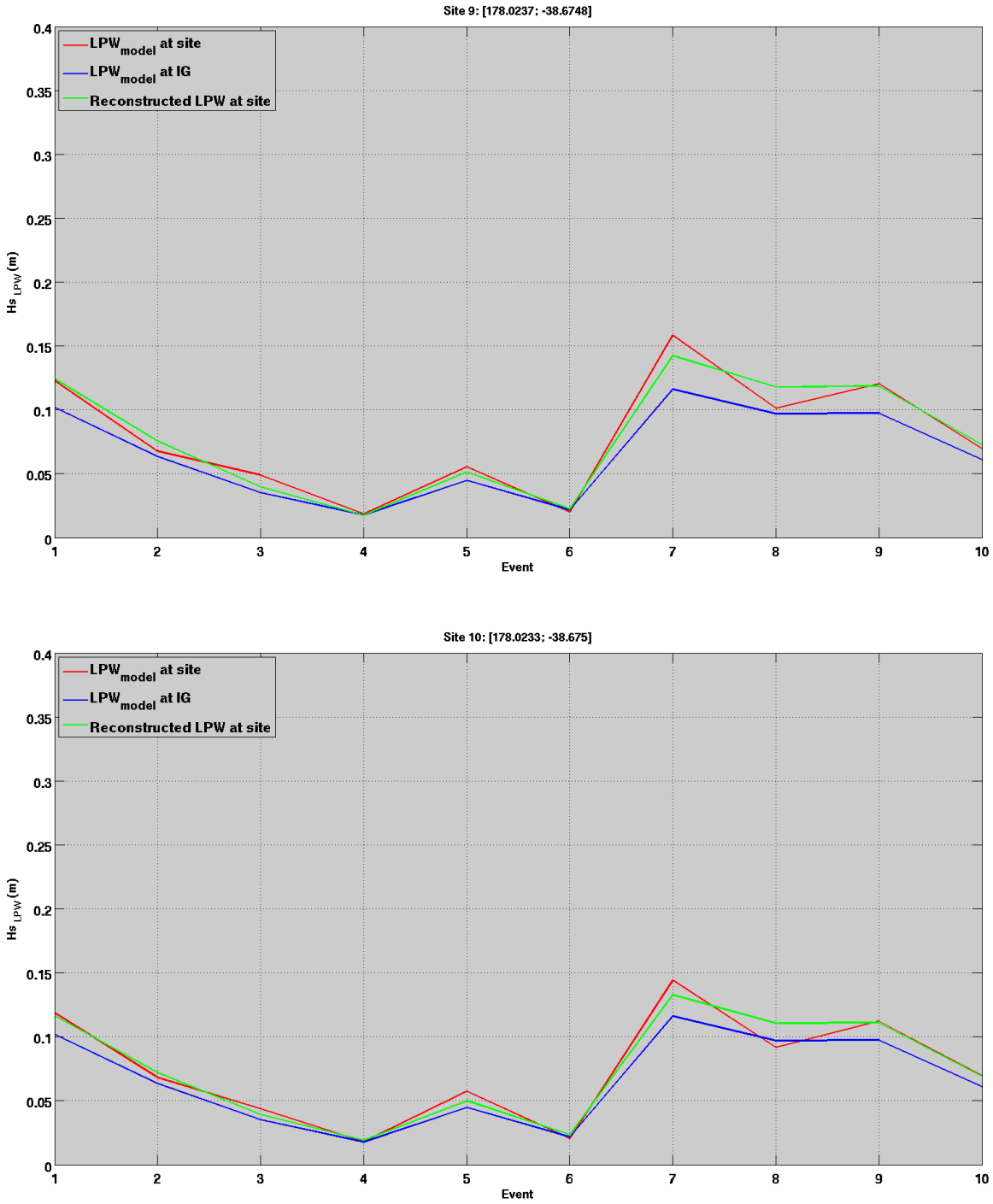


Figure 3.5 Model and reproduced $H_{s\ (LPW)}$ at Sites 9 and 10 for a total of 10 events (5 events at high and low tides) obtained from the Boussinesq wave model and the Equation 2.2, respectively,. The blue line indicates the model $H_{s\ (LPW)}$ at Site IG used in Equation 2.2.

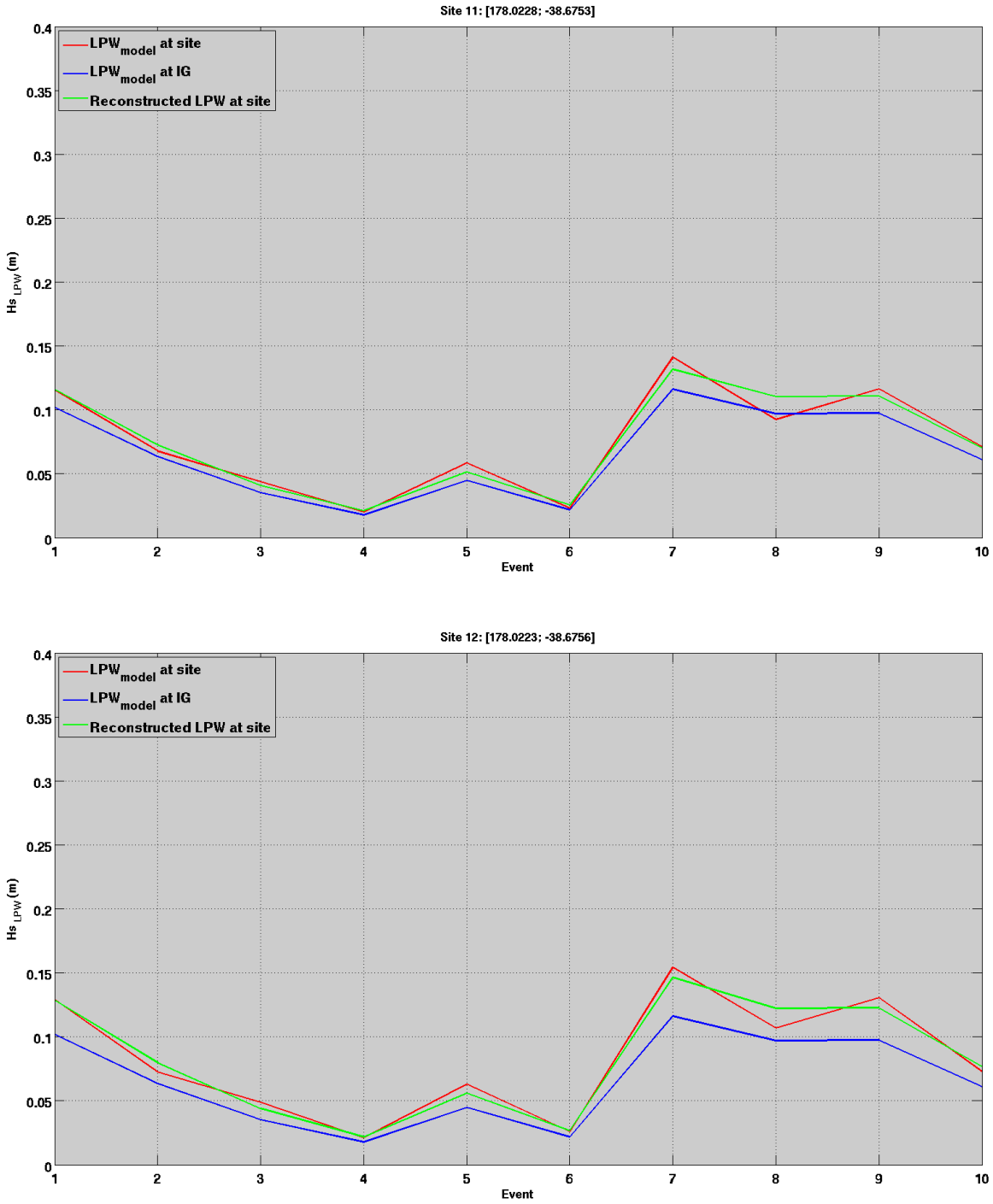


Figure 3.6 Model and reproduced $H_{s\ (LPW)}$ at Sites 11 and 12 for a total of 10 events (5 events at high and low tides) obtained from the Boussinesq wave model and the Equation 2.2, respectively,. The blue line indicates the model $H_{s\ (LPW)}$ at Site IG used in Equation 2.2.

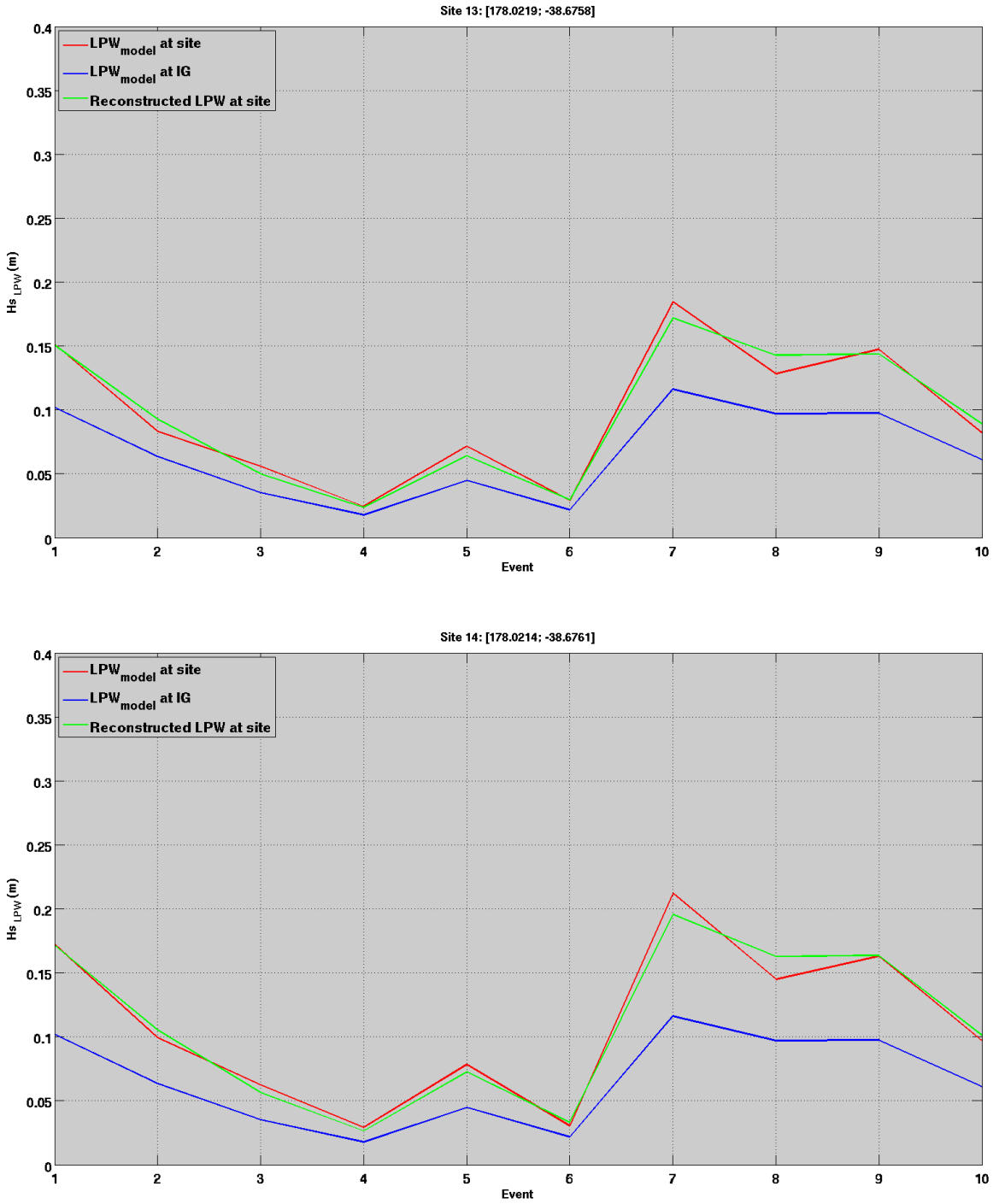


Figure 3.7 Model and reproduced $H_{s\ (LPW)}$ at Sites 13 and 14 for a total of 10 events (5 events at high and low tides) obtained from the Boussinesq wave model and the Equation 2.2, respectively,. The blue line indicates the model $H_{s\ (LPW)}$ at Site IG used in Equation 2.2.

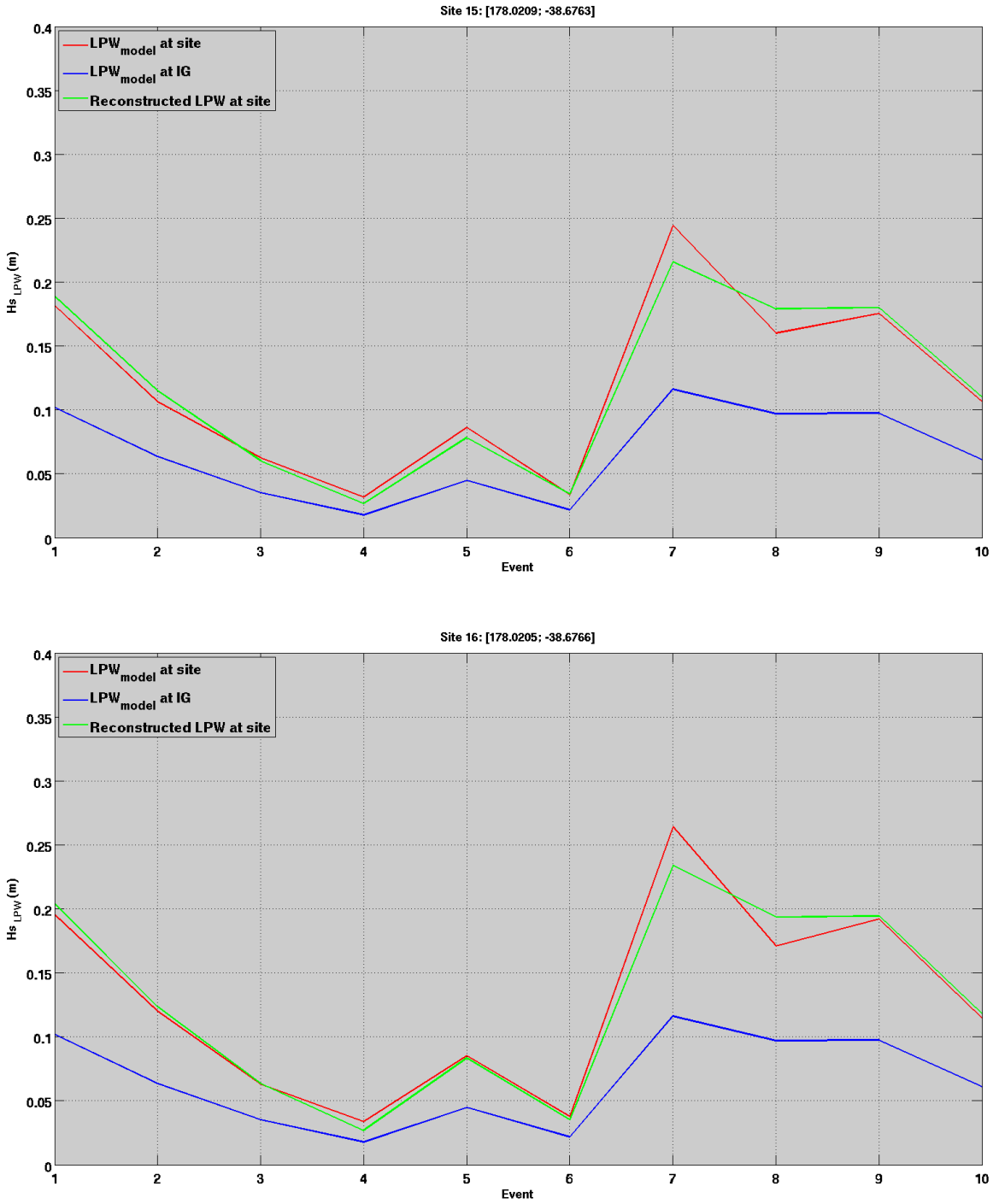


Figure 3.8 Model and reproduced $H_{s\ (LPW)}$ at Sites 15 and 16 for a total of 10 events (5 events at high and low tides) obtained from the Boussinesq wave model and the Equation 2.2, respectively,. The blue line indicates the model $H_{s\ (LPW)}$ at Site IG used in Equation 2.2.

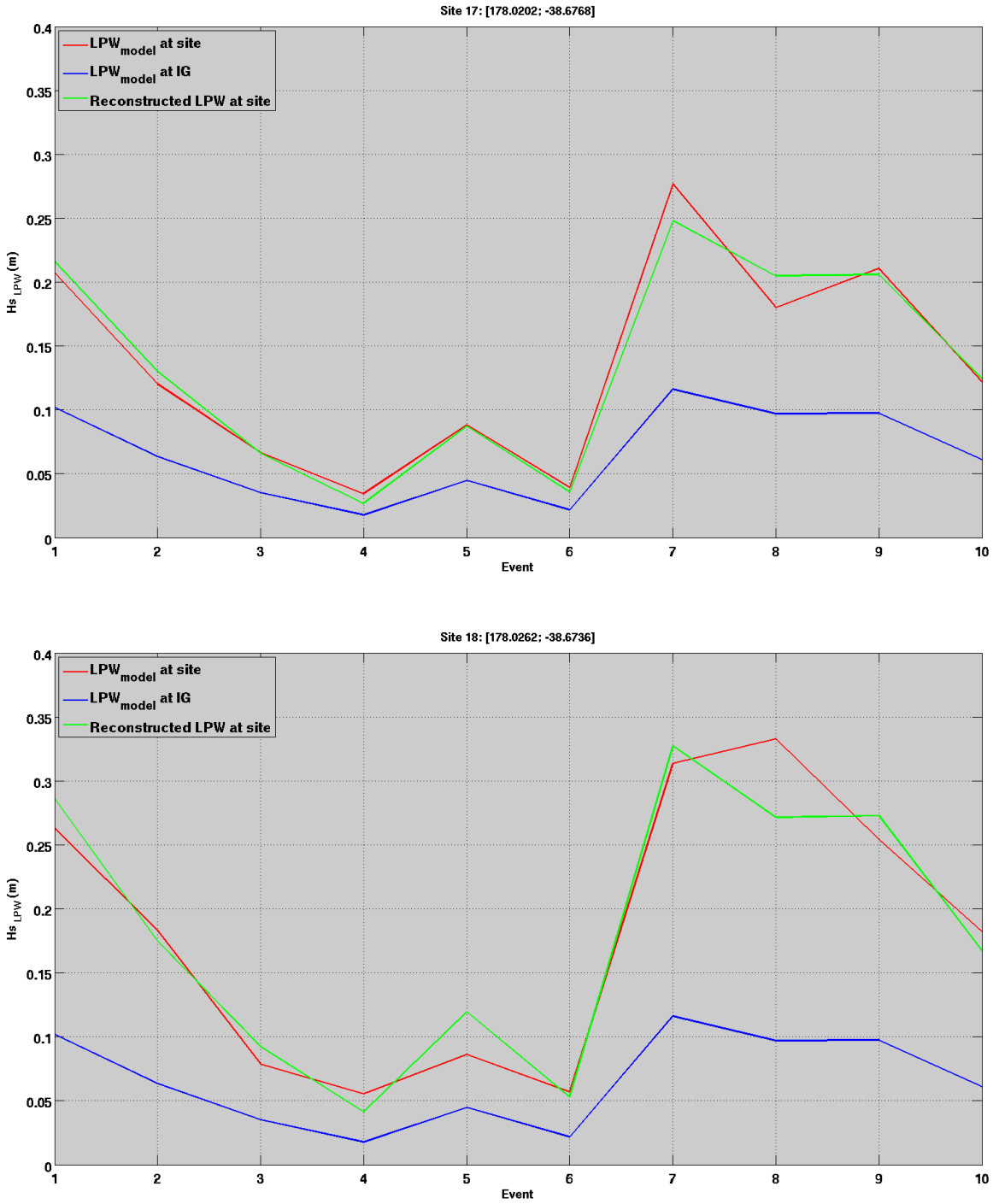


Figure 3.9 Model and reproduced $H_{s\ (LPW)}$ at Sites 17 and 18 for a total of 10 events (5 events at high and low tides) obtained from the Boussinesq wave model and the Equation 2.2, respectively,. The blue line indicates the model $H_{s\ (LPW)}$ at Site IG used in Equation 2.2.

## 3.2. Empirical equations to predict LPW along berth from offshore wave conditions at Site WB.

The coefficient *a1* was introduced in the previously established Eq. 2.1 at Site IG. This process consisted in multiplying the coefficients *b2* and *b5* by *a1* while *b1*, *b3* and *b4* remained unchanged. The empirical equations associated with Sites 1 to 18 are provided in Table 3.2.

Table 3.2 Empirical equations at Sites 1 to 18 and IG based on the offshore wave conditions.

| $Hs_{(LPW)} = (1+b1 \times tide) \times (b2 \times Hs_{(swell)}^{b3} \times Tp^{b4} + b5)$ | | | | | | | |
|---|---|---|---|---|---|---|---|
| **Position** | **Longitude (E)** | **Latitude (N)** | **Coefficient** | | | | |
| | | | **b1** | **b2** | **b3** | **b4** | **b5** |
| Ref IG | 178.022110 | -38.675000 | 0.54 | 0.011 | 1.1 | 0.5 | 0.025 |
| 1 | 178.027517 | -38.672717 | 0.54 | 0.0399 | 1.1 | 0.5 | 0.0906 |
| 2 | 178.027048 | -38.672983 | 0.54 | 0.0396 | 1.1 | 0.5 | 0.0899 |
| 3 | 178.026571 | -38.673242 | 0.54 | 0.0375 | 1.1 | 0.5 | 0.0853 |
| 4 | 178.026104 | -38.673496 | 0.54 | 0.0318 | 1.1 | 0.5 | 0.0724 |
| 5 | 178.025626 | -38.673755 | 0.54 | 0.0259 | 1.1 | 0.5 | 0.0589 |
| 6 | 178.025154 | -38.674012 | 0.54 | 0.0215 | 1.1 | 0.5 | 0.049 |
| 7 | 178.024682 | -38.674268 | 0.54 | 0.0176 | 1.1 | 0.5 | 0.0399 |
| 8 | 178.024215 | -38.674522 | 0.54 | 0.0158 | 1.1 | 0.5 | 0.0358 |
| 9 | 178.023737 | -38.674781 | 0.54 | 0.014 | 1.1 | 0.5 | 0.0317 |
| 10 | 178.023265 | -38.675037 | 0.54 | 0.0127 | 1.1 | 0.5 | 0.0289 |
| 11 | 178.022798 | -38.675291 | 0.54 | 0.0124 | 1.1 | 0.5 | 0.0281 |
| 12 | 178.022321 | -38.675551 | 0.54 | 0.0139 | 1.1 | 0.5 | 0.0316 |
| 13 | 178.021861 | -38.675813 | 0.54 | 0.0166 | 1.1 | 0.5 | 0.0377 |
| 14 | 178.021396 | -38.676077 | 0.54 | 0.0189 | 1.1 | 0.5 | 0.043 |
| 15 | 178.020926 | -38.676345 | 0.54 | 0.0212 | 1.1 | 0.5 | 0.0482 |
| 16 | 178.020462 | -38.676609 | 0.54 | 0.0231 | 1.1 | 0.5 | 0.0526 |
| 17 | 178.020194 | -38.676761 | 0.54 | 0.0247 | 1.1 | 0.5 | 0.0562 |
| 18 | 178.026200 | -38.673600 | 0.54 | 0.032 | 1.1 | 0.5 | 0.0726 |

## 3.3. LPW climate along berth

The LPW climate was reconstructed at Sites 1 to 18 using nowcast data as inputs for the empirical equations presented in Figure 3.10 to Figure 3.18. The time series of $H_{s(LPW)}$ are shown in Figure 3.10 - Figure 3.18, while corresponding LPW statistics are provided in Table 3.3.

Table 3.3 LPW statistics based on the reconstructed LPW climate at Sites 1 to 18 applying the empirical equations from nowcast data.

| Position | Longitude (E) | Latitude (N) | LPW statistics (m) | | | | |
|---|---|---|---|---|---|---|---|
| | | | mean | P50 | P95 | P99 | max |
| 1 | 178.027517 | -38.672717 | 0.08 | 0.07 | 0.15 | 0.21 | 0.40 |
| 2 | 178.027048 | -38.672983 | 0.28 | 0.25 | 0.51 | 0.73 | 1.00 |
| 3 | 178.026571 | -38.673242 | 0.28 | 0.25 | 0.51 | 0.72 | 1.00 |
| 4 | 178.026104 | -38.673496 | 0.26 | 0.23 | 0.48 | 0.69 | 1.00 |
| 5 | 178.025626 | -38.673755 | 0.22 | 0.20 | 0.41 | 0.59 | 0.98 |
| 6 | 178.025154 | -38.674012 | 0.18 | 0.16 | 0.33 | 0.49 | 0.93 |
| 7 | 178.024682 | -38.674268 | 0.15 | 0.13 | 0.27 | 0.40 | 0.77 |
| 8 | 178.024215 | -38.674522 | 0.12 | 0.11 | 0.22 | 0.33 | 0.63 |
| 9 | 178.023737 | -38.674781 | 0.11 | 0.09 | 0.20 | 0.29 | 0.56 |
| 10 | 178.023265 | -38.675037 | 0.10 | 0.09 | 0.18 | 0.26 | 0.50 |
| 11 | 178.022798 | -38.675291 | 0.09 | 0.08 | 0.17 | 0.24 | 0.46 |
| 12 | 178.022321 | -38.675551 | 0.09 | 0.08 | 0.16 | 0.24 | 0.45 |
| 13 | 178.021861 | -38.675813 | 0.10 | 0.09 | 0.18 | 0.26 | 0.50 |
| 14 | 178.021396 | -38.676077 | 0.12 | 0.11 | 0.22 | 0.31 | 0.60 |
| 15 | 178.020926 | -38.676345 | 0.13 | 0.12 | 0.25 | 0.36 | 0.68 |
| 16 | 178.020462 | -38.676609 | 0.15 | 0.13 | 0.27 | 0.40 | 0.76 |
| 17 | 178.020194 | -38.676761 | 0.16 | 0.14 | 0.29 | 0.43 | 0.83 |
| 18 | 178.026200 | -38.673600 | 0.17 | 0.15 | 0.31 | 0.46 | 0.88 |

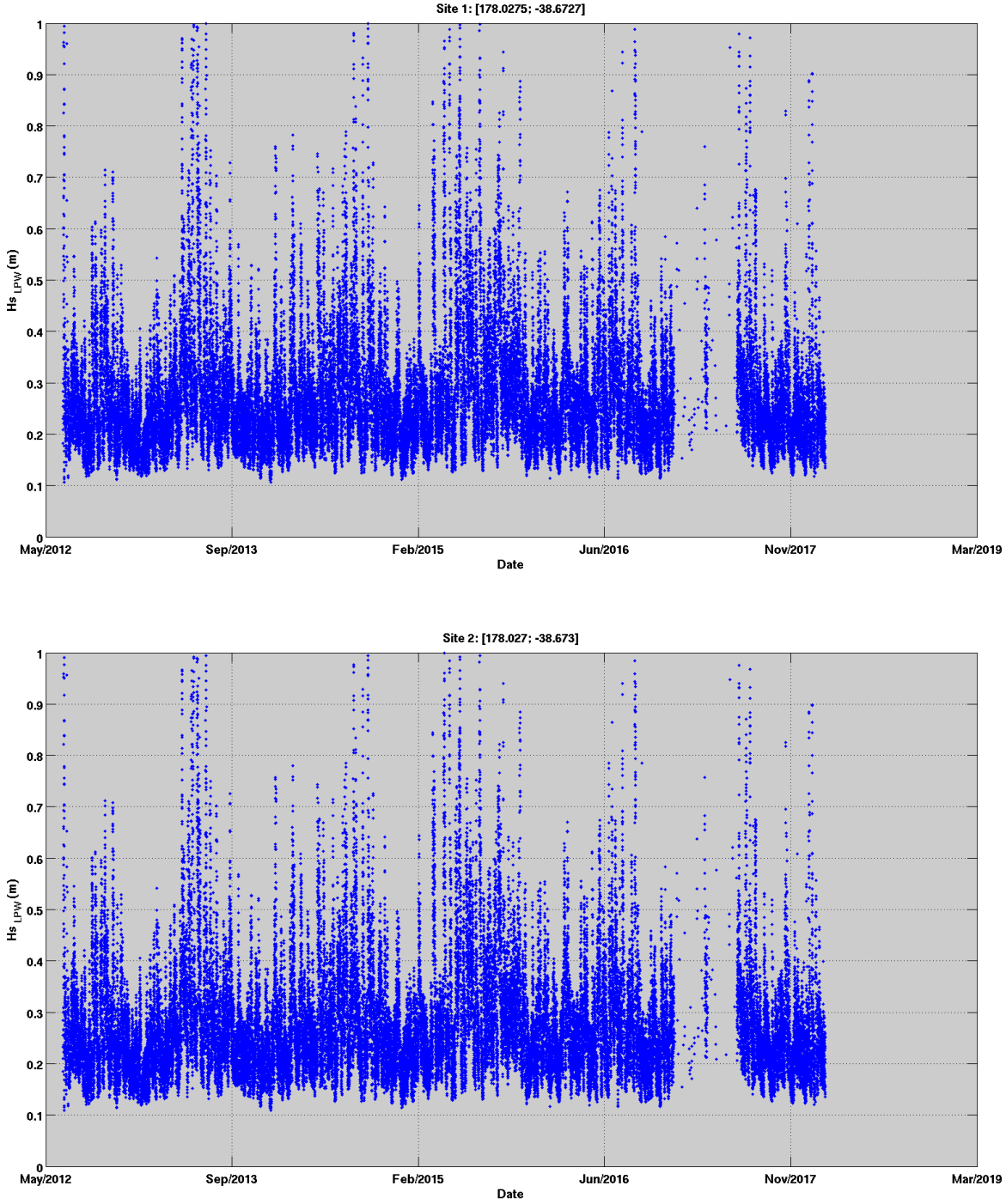


Figure 3.10 $H_{s\ (LPW)}$ at Sites 1 and 2 predicted using their respective empirical LPW equation defined in Table 3.2.

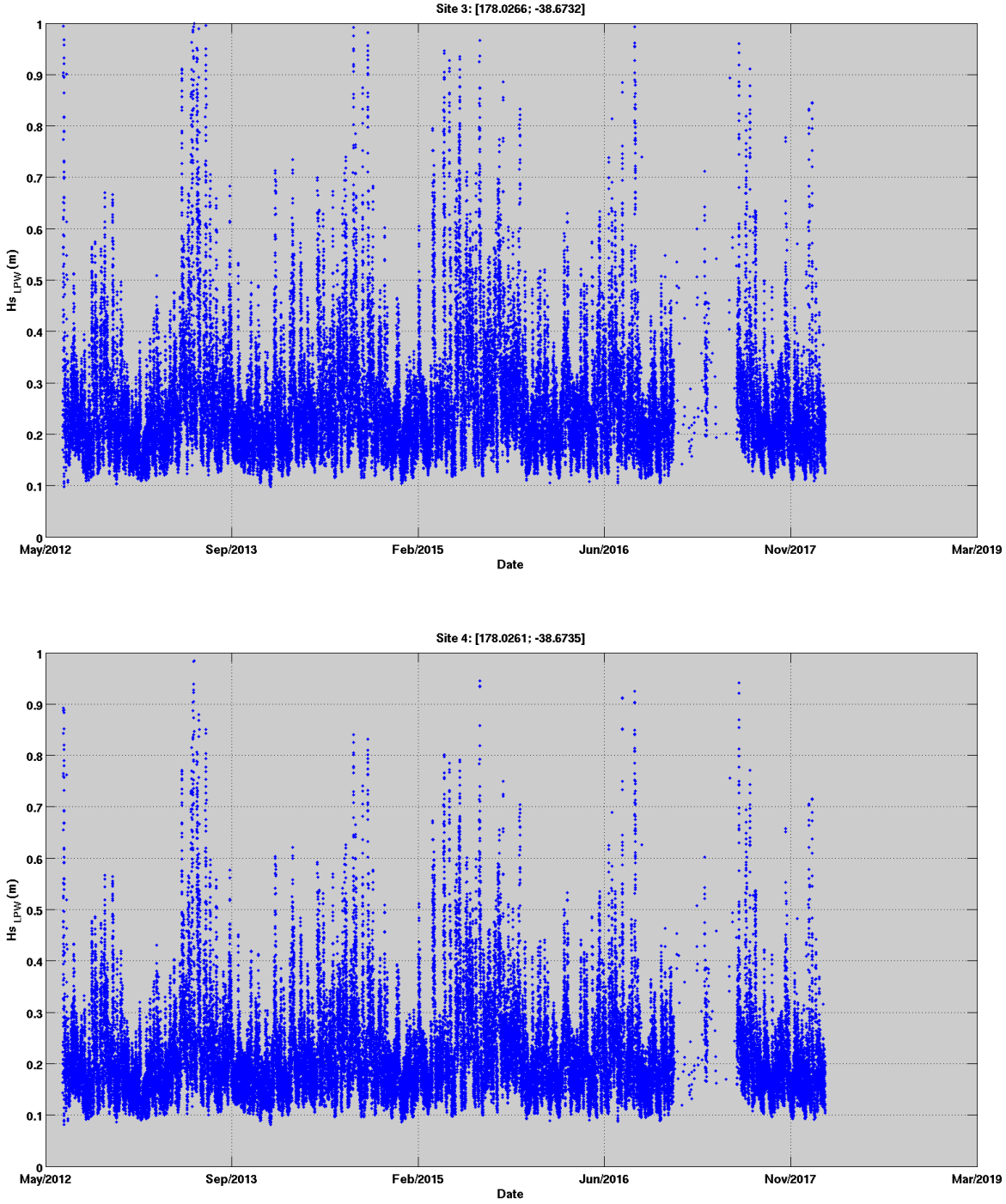


Figure 3.11 $H_{s\ (LPW)}$ at Sites 3 and 4 predicted using their respective empirical LPW equation defined in Table 3.2.

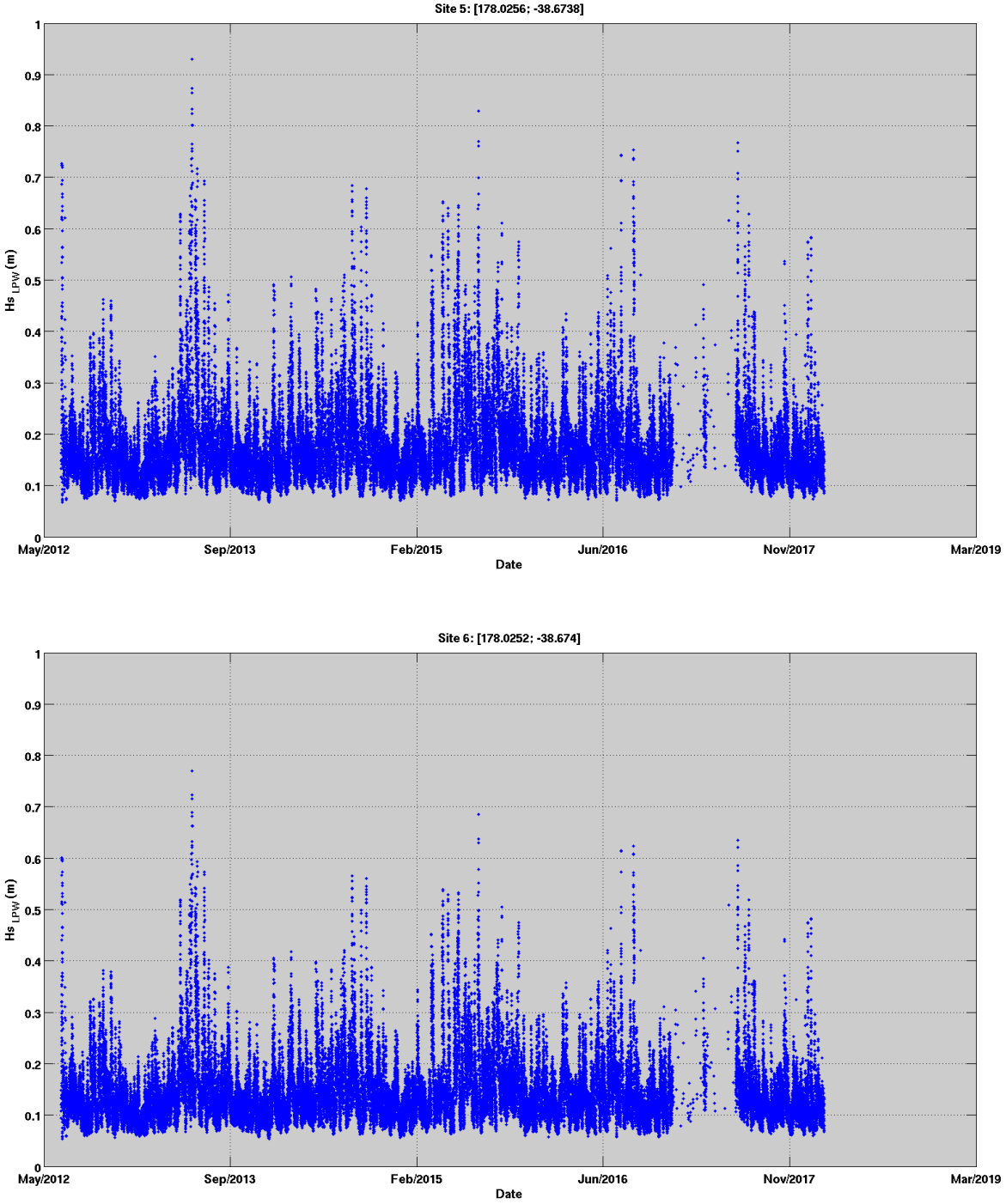


Figure 3.12 $H_{s\ (LPW)}$ at Sites 5 and 6 predicted using their respective empirical LPW equation defined in Table 3.2.

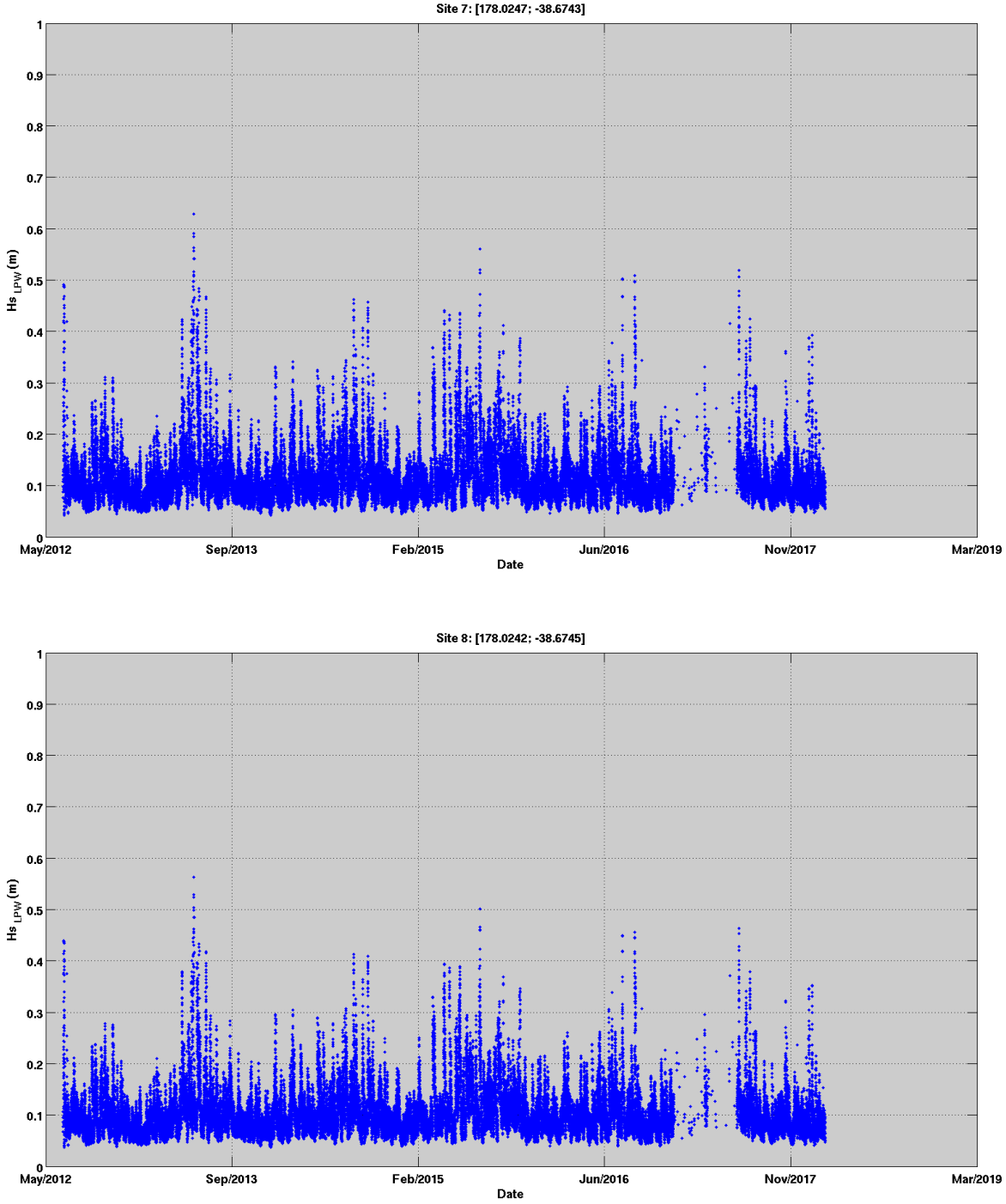


Figure 3.13 $H_{s\ (LPW)}$ at Sites 7 and 8 predicted using their respective empirical LPW equation defined in Table 3.2.

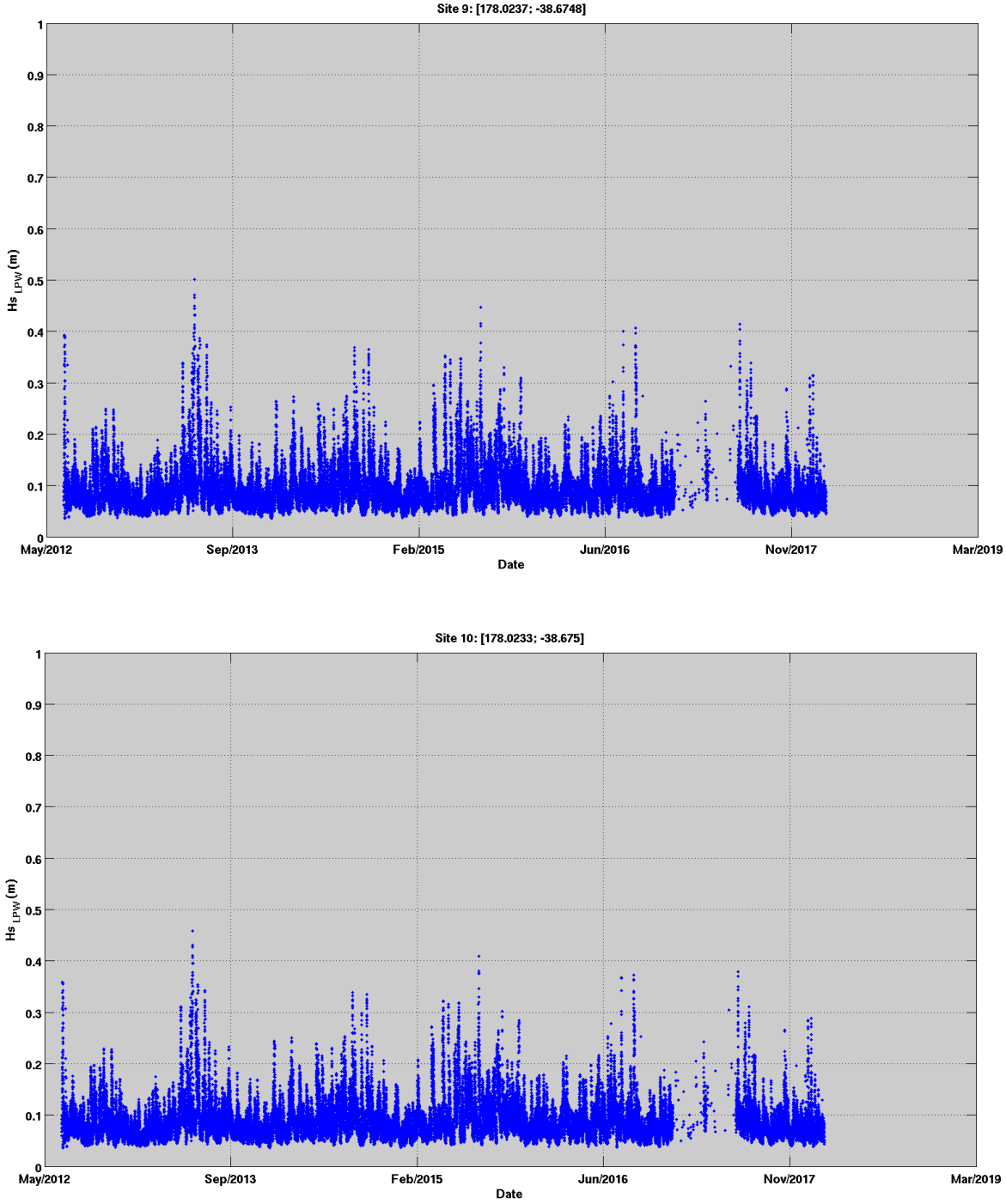


Figure 3.14 $H_{s\ (LPW)}$ at Sites 9 and 10 predicted using their respective empirical LPW equation defined in Table 3.2.

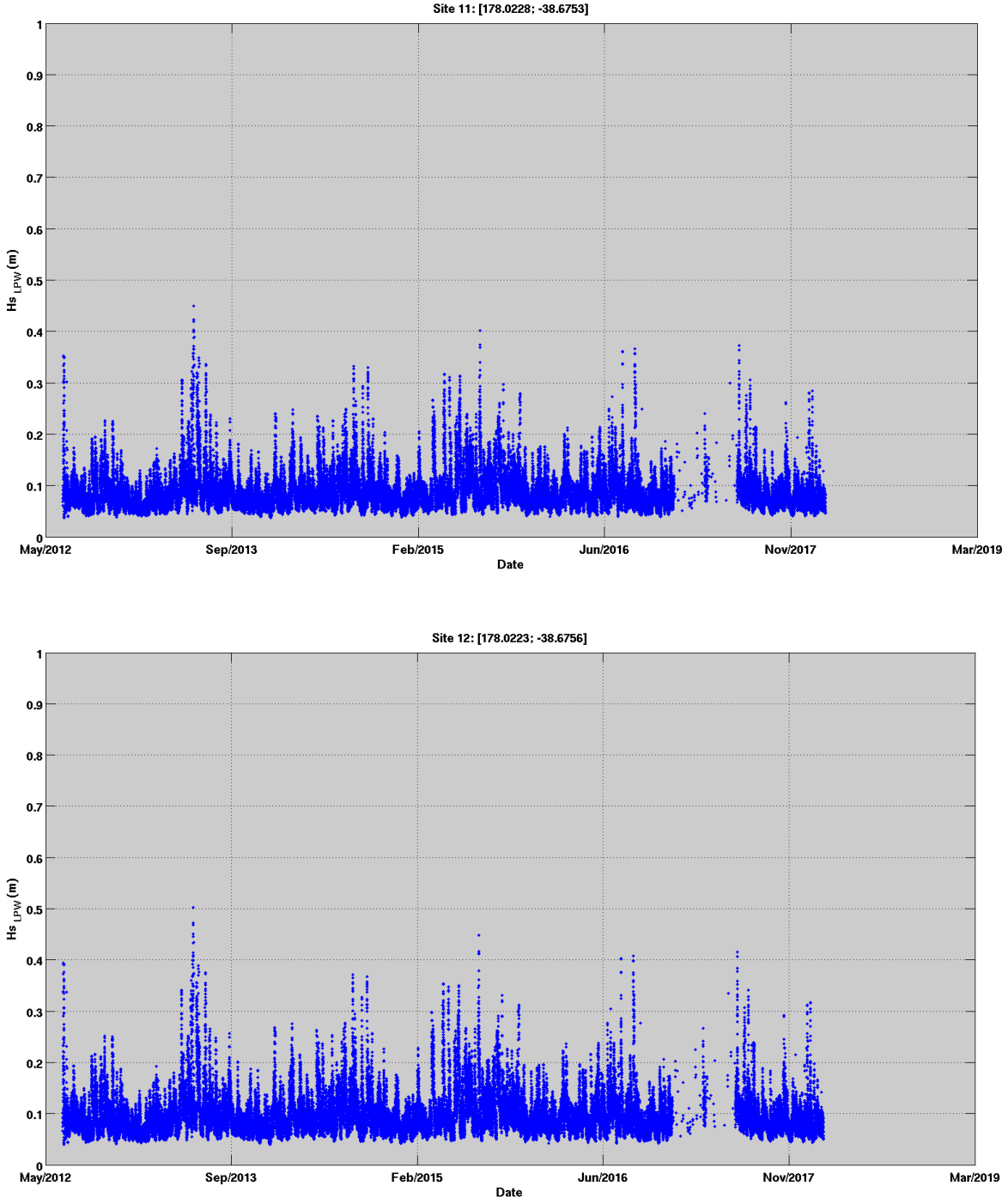


Figure 3.15 $H_{s\ (LPW)}$ at Sites 11 and 12 predicted using their respective empirical LPW equation defined in Table 3.2.

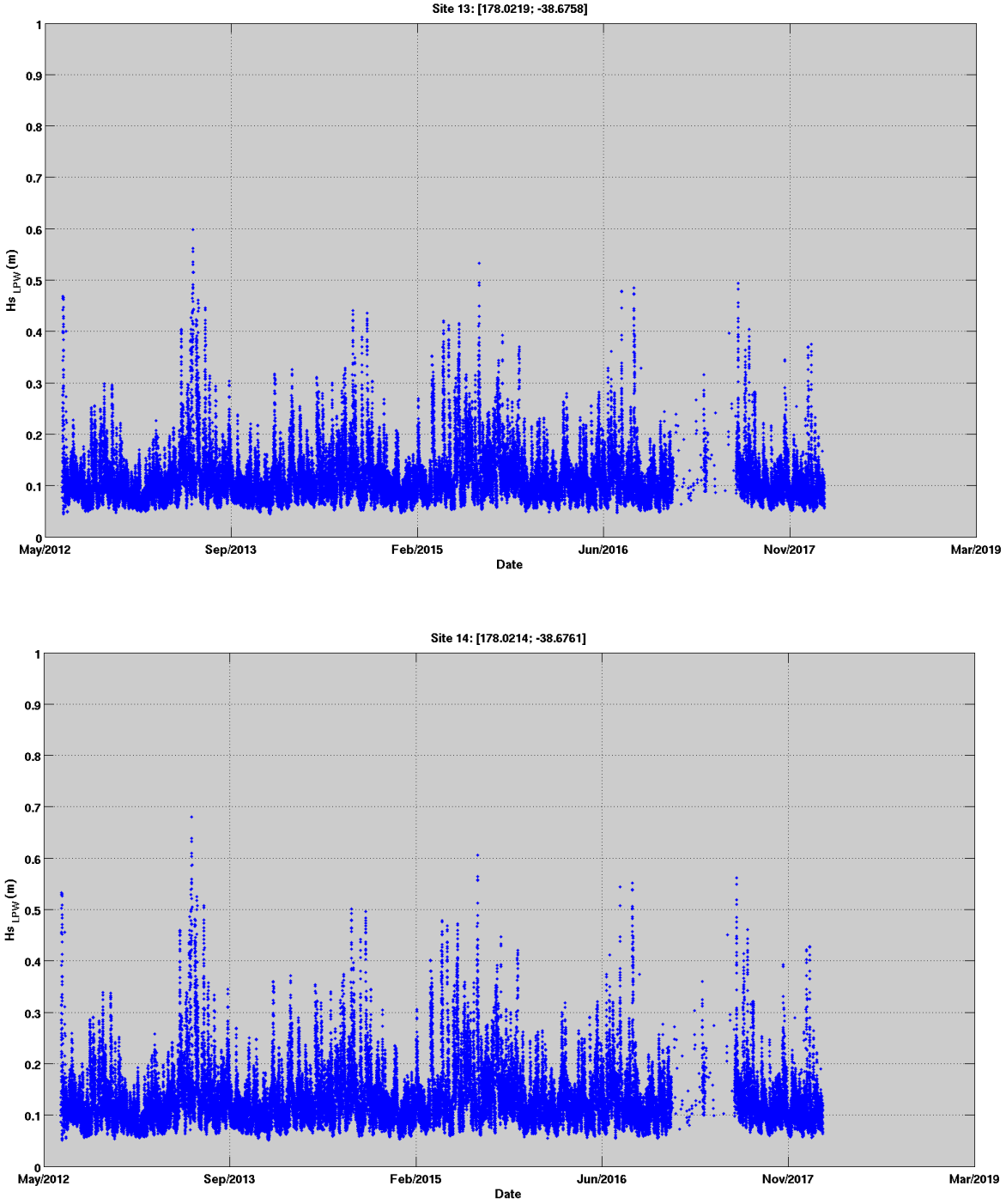


Figure 3.16 $H_{s\ (LPW)}$ at Sites 13 and 14 predicted using their respective empirical LPW equation defined in Table 3.2.

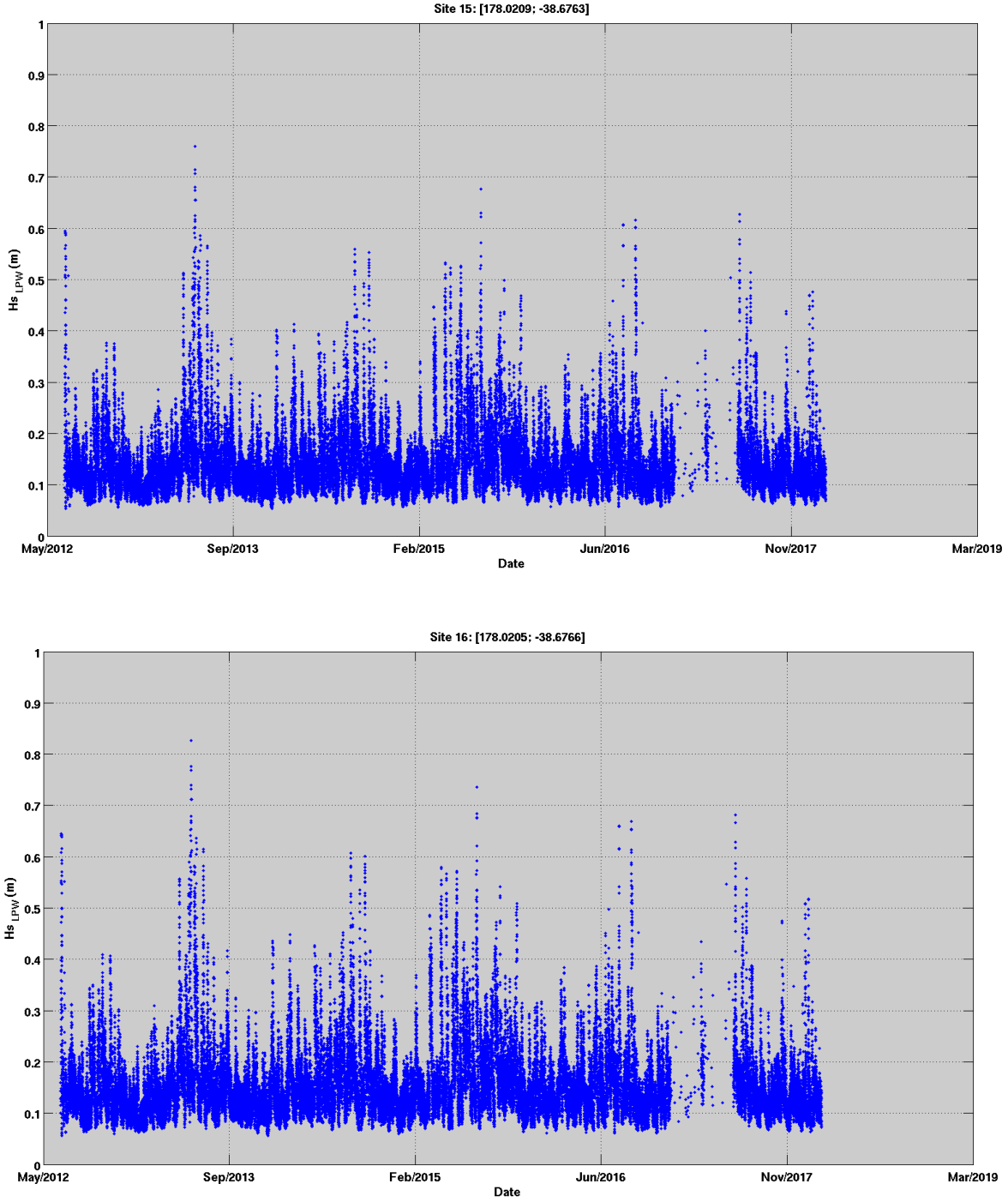


Figure 3.17 $H_{s\ (LPW)}$ at Sites 15 and 16 predicted using their respective empirical LPW equation defined in Table 3.2.

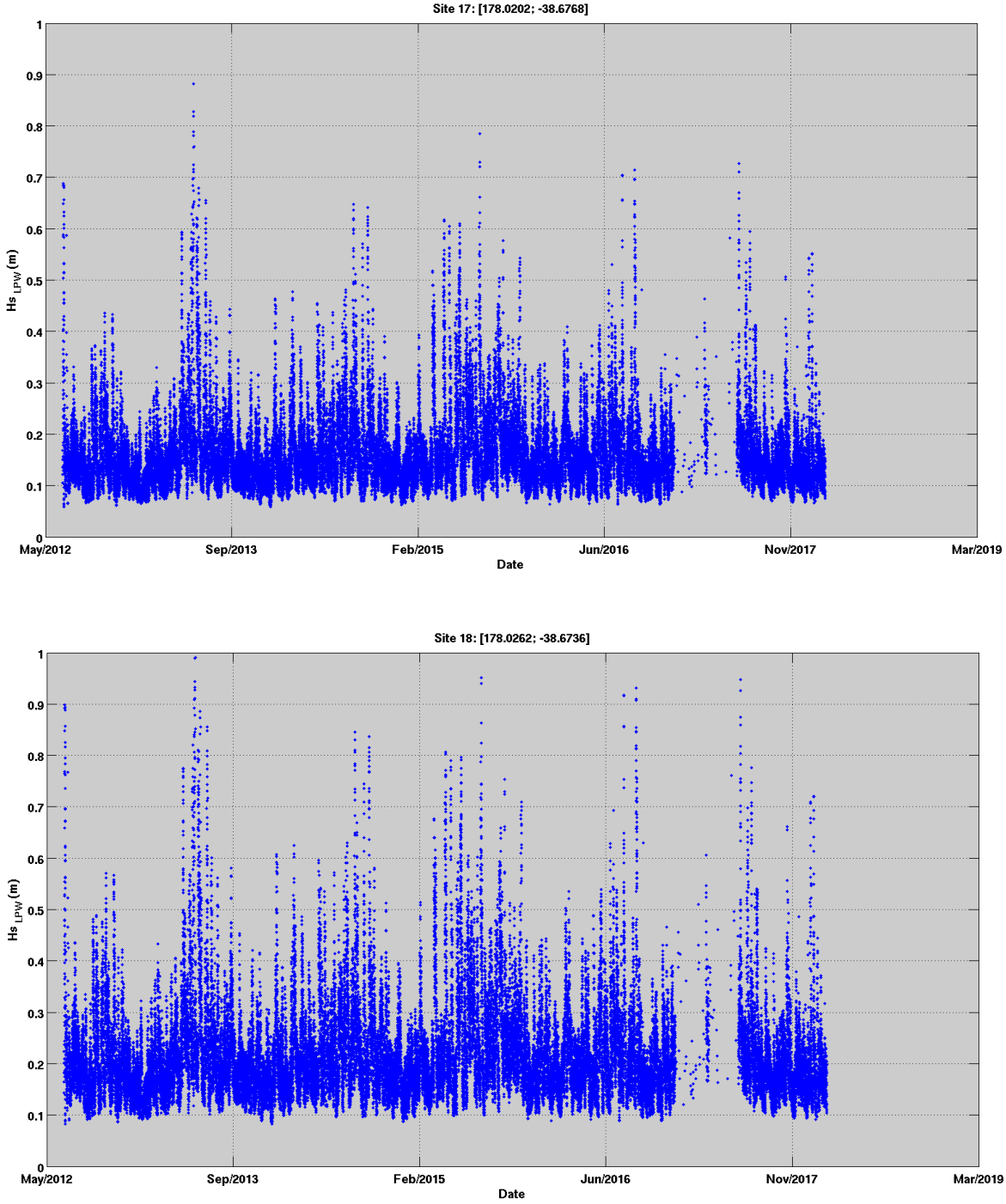


Figure 3.18 $H_{s\ (LPW)}$ at Sites 17 and 18 predicted using their respective empirical LPW equation defined in Table 3.2.

# 4. CAVEATS OF APPROACH

The empirical equations proposed in the present study have been determined using 10 wave scenarios simulated with the Boussinesq numerical model, 5 each at high and low water tidal elevations. The limited number of data points with which to derive the empirical relationship used to define the LPW wave climate at the sites of interest introduces a degree of uncertainty into the derived relationships. This uncertainty needs to be considered when applying the derived results.

MOS preferred method for deriving LPW relationships is to consider at least one month of measured data at the several sites of interest and derive more robust statistically relevant empirical relationships between either the measured wave climate or modelled nowcast offshore wave climate and the inner harbour LPW.

# 5. SUMMARY

A set of 18 empirical equations has been established to predict the long period wave (LPW) climate along berth based on the offshore wave climate and the tidal variation. Outputs from 10 scenarios simulated with the Boussinesq wave model FUNWAVE has been examined to rescale the existing equation applied in the forecast system to taking into account the spatial variability of the LPW field within the harbour (5 at high tide and 5 at low tide).

Offshore nowcast data produced by MetOcean Solutions between 2012 and 2017 have been used as inputs for the new established empirical equations at berth sites to reproduce the LPW climate over this period. LPW statistics specific to each site have been calculated.

The limited number of simulations has been considered, and this infers some caveats to the approach used.

# 6. REFERENCES

Holthuijsen, L.H., 2010. Waves in oceanic and coastal waters. Cambridge university press.

MetOcean Solutions, 2013. Long period wave modelling, Boussinesq modelling of short and long period wave energy at Eastland Port. Report prepared for Eastland Port.

Thomson, J., Elgar, S., Raubenheimer, B., Herbers, T.H.C., Guza, R.T., 2006. Tidal modulation of infragravity waves via nonlinear energy losses in the surfzone. Geophys. Res. Lett. 33.

# APPENDIX A.

Table A.1 Ratio Hs(swell) / Hs(swell WB) from FUNWAVE outputs extracted at 19 sites.

| Position | Longitude (E) | Latitude (N) | Ratio $Hs_{(swell)}$ / $Hs_{(swell\ WB)}$ at MHWS | | | | |
|---|---|---|---|---|---|---|---|
| | | | Event1 | Event2 | Event3 | Event4 | Event5 |
| **IG** | 178.022110 | -38.675000 | 0.16 | 0.12 | 0.09 | 0.12 | 0.15 |
| **1** | 178.027517 | -38.672717 | 0.09 | 0.06 | 0.04 | 0.07 | 0.09 |
| **2** | 178.027048 | -38.672983 | 0.09 | 0.07 | 0.04 | 0.07 | 0.09 |
| **3** | 178.026571 | -38.673242 | 0.09 | 0.07 | 0.05 | 0.07 | 0.09 |
| **4** | 178.026104 | -38.673496 | 0.07 | 0.04 | 0.03 | 0.04 | 0.07 |
| **5** | 178.025626 | -38.673755 | 0.10 | 0.09 | 0.06 | 0.10 | 0.09 |
| **6** | 178.025154 | -38.674012 | 0.10 | 0.08 | 0.07 | 0.08 | 0.10 |
| **7** | 178.024682 | -38.674268 | 0.16 | 0.13 | 0.09 | 0.12 | 0.16 |
| **8** | 178.024215 | -38.674522 | 0.16 | 0.11 | 0.09 | 0.12 | 0.17 |
| **9** | 178.023737 | -38.674781 | 0.15 | 0.15 | 0.10 | 0.15 | 0.15 |
| **10** | 178.023265 | -38.675037 | 0.16 | 0.13 | 0.10 | 0.13 | 0.17 |
| **11** | 178.022798 | -38.675291 | 0.15 | 0.14 | 0.10 | 0.14 | 0.15 |
| **12** | 178.022321 | -38.675551 | 0.16 | 0.16 | 0.12 | 0.16 | 0.16 |
| **13** | 178.021861 | -38.675813 | 0.21 | 0.19 | 0.14 | 0.19 | 0.20 |
| **14** | 178.021396 | -38.676077 | 0.24 | 0.22 | 0.16 | 0.22 | 0.23 |
| **15** | 178.020926 | -38.676345 | 0.23 | 0.22 | 0.17 | 0.22 | 0.23 |
| **16** | 178.020462 | -38.676609 | 0.25 | 0.25 | 0.20 | 0.24 | 0.25 |
| **17** | 178.020194 | -38.676761 | 0.31 | 0.31 | 0.24 | 0.31 | 0.30 |
| **18** | 178.026200 | -38.673600 | 0.07 | 0.05 | 0.04 | 0.04 | 0.07 |
| **Position** | **Longitude (E)** | **Latitude (N)** | **Ratio $Hs_{(swell)}$ / $Hs_{(swell\ WB)}$ at MLWS** | | | | |
| **IG** | 178.022110 | -38.675000 | 0.14 | 0.10 | 0.07 | 0.11 | 0.14 |
| **1** | 178.027517 | -38.672717 | 0.08 | 0.04 | 0.03 | 0.05 | 0.08 |
| **2** | 178.027048 | -38.672983 | 0.08 | 0.05 | 0.03 | 0.06 | 0.09 |
| **3** | 178.026571 | -38.673242 | 0.09 | 0.06 | 0.04 | 0.06 | 0.09 |
| **4** | 178.026104 | -38.673496 | 0.06 | 0.03 | 0.03 | 0.04 | 0.07 |
| **5** | 178.025626 | -38.673755 | 0.09 | 0.07 | 0.04 | 0.07 | 0.09 |
| **6** | 178.025154 | -38.674012 | 0.08 | 0.07 | 0.06 | 0.08 | 0.08 |
| **7** | 178.024682 | -38.674268 | 0.16 | 0.11 | 0.07 | 0.11 | 0.16 |
| **8** | 178.024215 | -38.674522 | 0.12 | 0.10 | 0.07 | 0.12 | 0.13 |
| **9** | 178.023737 | -38.674781 | 0.17 | 0.13 | 0.09 | 0.13 | 0.16 |
| **10** | 178.023265 | -38.675037 | 0.16 | 0.13 | 0.09 | 0.13 | 0.16 |
| **11** | 178.022798 | -38.675291 | 0.15 | 0.14 | 0.10 | 0.14 | 0.15 |
| **12** | 178.022321 | -38.675551 | 0.18 | 0.15 | 0.11 | 0.16 | 0.18 |
| **13** | 178.021861 | -38.675813 | 0.22 | 0.19 | 0.14 | 0.20 | 0.22 |
| **14** | 178.021396 | -38.676077 | 0.24 | 0.22 | 0.17 | 0.22 | 0.24 |
| **15** | 178.020926 | -38.676345 | 0.25 | 0.22 | 0.17 | 0.23 | 0.25 |
| **16** | 178.020462 | -38.676609 | 0.27 | 0.25 | 0.21 | 0.25 | 0.27 |
| **17** | 178.020194 | -38.676761 | 0.34 | 0.32 | 0.26 | 0.33 | 0.33 |
| **18** | 178.026200 | -38.673600 | 0.06 | 0.04 | 0.03 | 0.04 | 0.06 |